

Effect of high substrate bias and hydrogen and nitrogen incorporation on density of states and field-emission threshold in tetrahedral amorphous carbon films

O. S. Panwar^{a)} and M. A. Khan

Plasma Processed Materials Group, National Physical Laboratory, Dr. K. S. Krishnan Road, New Delhi 110 012, India

B. S. Satyanarayana

40, Sreeniketan, NDSE 24, Vasundhara Enclave, New Delhi 110096, India

R. Bhattacharyya

National Physical Laboratory, New Delhi 110012, India

B. R. Mehta

Department of Physics, Indian Institute of Technology, Hauz Khas, New Delhi 110016, India

S. Kumar and Ishpal

Plasma Processed Materials Group, National Physical Laboratory, Dr. K. S. Krishnan Road, New Delhi 110 012, India

(Received 15 July 2009; accepted 8 February 2010; published 31 March 2010)

This article reports the influence of substrate bias during growth and of hydrogen and nitrogen incorporation on density of states $[N(E_F)]$ and field-emission threshold ($E_{\text{turn-on}}$) in tetrahedral amorphous carbon (ta-C) films, deposited using an S-bend filtered cathodic vacuum arc process. The variation in negative substrate bias from -20 to -200 V was found to initially lead to a small decrease in $N(E_F)$ and $E_{\text{turn-on}}$, and a small increase in the emission current density (J) at 12.5 V/ μm in the case of as-grown ta-C films; beyond -200 V substrate bias there is a reversal in the trend. The values of $N(E_F)=1.3 \times 10^{17}$ cm $^{-3}$ eV $^{-1}$, $E_{\text{turn-on}}=8.3$ V/ μm , and $J=6.19$ mA/cm 2 were observed at -200 V substrate bias. However at -300 V the properties were not very different from those at -200 V substrate bias and so with a view to use the higher energy, hydrogen and nitrogen incorporation studies were carried out in this condition. It was observed that there was further enhancement in properties with hydrogen and nitrogen incorporation. The best properties measured with in the range of hydrogen and nitrogen incorporation in the present study were $N(E_F)=8.0 \times 10^{16}$ cm $^{-3}$ eV $^{-1}$, $E_{\text{turn-on}}=7.6$ V/ μm , and $J=23.7$ mA/cm 2 , respectively. © 2010 American Vacuum Society. [DOI: 10.1116/1.3359586]

I. INTRODUCTION

Amorphous carbon films having a high sp^3 bonded carbon content, referred to as tetrahedral amorphous carbon (ta-C), have attracted considerable interest due to their unique mechanical, structural, and morphological properties.¹⁻⁶ Field emission from carbon-based cold cathodes has been of great technological and fundamental interests due to its possible application in display devices and vacuum microelectronics.⁶ The study of tetrahedral amorphous carbon films to date has shown that the films are not very useful for electronic applications. However, now there is an increasing interest in use of ta-C based material in other electronic and microelectronic applications including applications such as sensors, micro-electromechanical systems (MEMS), and dielectrics layer in ULSI.^{7,8} Hence, there is a need to study and further understand the electrical and electronic properties of ta-C films, including the density of states within the energy gap. There are several factors that determine the density of states of a

given material, the most important being the interatomic distance, coordination number, and type of chemical bonds. In ta-C, as in other diamondlike carbon, the sp^3 sites contribute to σ bonds while the sp^2 sites form both the σ and π bonds. The π states being near to the Fermi level thus control the electronic properties significantly. These ta-C films have been grown using a wide variety of processes, including filtered cathodic vacuum arc (FCVA) direct and pulsed source, pulsed-laser ablation, mass selected ion-beam deposition, and electron cyclotron wave-resonance processes, and there are many good reviews covering these in literature.^{2-4,9} Among the successful methods for preparing ta-C films, the FCVA technique is of particular interest for industrial applications because it provides highly ionized plasma of energetic carbon ions, from which dense films of amorphous carbon can be grown at reasonable deposition rates, at lower temperature on inexpensive substrates including glass and plastics over large area.¹⁰

The cathodic arc uses relatively low voltage and high current density of discharge, in which the macroscopic fragments of the cathode material are also emitted. Electromagnetic deflection of the plasma through L bend (90°) using a

^{a)}Author to whom correspondence should be addressed; electronic mail: ospanwar@mail.nplindia.ernet.in

curved solenoid was first used to remove the macro particles from the carbon plasma by Aksenov *et al.*¹¹ The macroparticle filter, on the other hand, has limited transport efficiency and tends to collimate the plasma, leading to a restricted area of deposition. The efficiency of the removal of macroparticles can also be improved using an *S*-bend magnetic filter, although it decreases the deposition rates due to reduced ion-transport efficiency.^{12–17} The pulsed mode of the plasma also allows better filtering of the macroparticle because the ions tend to be entrained in the plasma beam during the pulse but fall out of the plasma when the beam stops.^{18–22} All these processes mentioned above are highly energetic processes, and the control of ion energy leads to the variation in the material properties. Further, the high rate of ionization and the option to vary the ion energy and ion density can, under optimum conditions, lead to the creation of momentary pseudothermodynamic conditions of high temperature, on the surface of the film, leading to nanostructured carbons.^{23,24} Thus, very subtle variation in the process parameters leads to variation in the material properties. However, there are only a few reports on the properties of carbon thin films deposited by FCVA processes using an *S*-bend magnetic filter and practically no reports on the systematic study of carbon films grown at higher ion energies. We believe the study of carbon films under varying conditions of hydrogen and nitrogen grown at higher deposition ion energies or substrate bias could be very significant, especially with the increased interest in nanostructured carbons for diverse applications hence we report the study of ta-C films grown at a substrate bias of -300 V under varying conditions of hydrogen and nitrogen. The properties investigated are also system dependent.² One of the first systematic reports of ta-C films at high substrate bias (-300 V) of reflectance and photoluminescence,²⁵ x-ray photoelectron spectroscopy (XPS), x-ray Auger induced electron spectroscopy (XAES), and Raman spectroscopy studies,²⁶ plasma diagnostic studies²⁷ and electrical and mechanical properties²⁸ have been published recently. The current work complements it, especially with reference to the possibility of use of this material as electronic material by studying the defect density measured using space-charge-limited-conduction (SCLC) studies and the field assisted electron emission of as-grown ta-C, ta-C:H, and ta-C:N films. To our knowledge, this is one of the first studies to report a correlation between density of states, sp^3 content, and microstructure of the films, and field assisted emission characteristics from hydrogen and nitrogen incorporation on carbon films grown using the FCVA process, at high substrate bias voltages of the order of -300 V.

II. EXPERIMENTAL DETAILS

The ta-C films under varying conditions of substrate bias (-20 to -450 V) and hydrogen (partial pressure varied from 1.2×10^{-5} to 1.4×10^{-3} mbar) and nitrogen (partial pressure varied from 1.2×10^{-5} to 3.0×10^{-3} mbar) incorporation were deposited using a custom-built double-bend (*S* bend) FCVA process on cleaned, highly conducting *n*- and *p*-type silicon wafers (of resistivity 0.001 – 0.005 Ω cm). The de-

tails about the FCVA system and the other deposition conditions have been described earlier.^{25–28} During the deposition of ta-C:H and ta-C:N films, the substrate bias was kept constant at -300 V and the arc current (~ 75 A) and magnetic field (~ 350 G) in the *S*-bend duct were also kept constant. The thickness of the films is found to be in the range of 500 ± 100 Å as measured by a Talystep (Rank Taylor and Hobson) thickness profiler. *I*-*V* characteristics were investigated on sandwiched specimens prepared by depositing as-grown ta-C films and ta-C:H films on p^{++} silicon substrates, and ta-C:N films on n^{++} silicon substrates and aluminum dots have subsequently been deposited as a top electrode by thermal evaporation at $\sim 10^{-6}$ mbar vacuum. The active area of the devices was ~ 0.04 cm² and a Keithley 610 C Solid-State Electrometer was used for the *I*-*V* measurements. The *I*-*V* measurements were carried out by reversing the polarity of voltage applied. It may be mentioned that Ohmic behavior was observed with both the positive and negative polarity of the voltage applied and similar *I*-*V* characteristics were also recorded in typical range of fields used, which were repeatable on the same dot and on set of dots also. There were also some points that got shorted, even before the *I*-*V* measurements because of the macroparticle induced holes. However, the study was repeated over a set of points to make sure that the measurements were repeatable. Thus, the SCLC measurements are a reasonable representation of the nature of the films being studied. The field-emission measurements were carried out using a parallel-plate configuration. An indium tin oxide-coated glass substrate was used as anode and diamondlike carbon (DLC)/ta-C films deposited on polished silicon substrates were used as the cathode. The samples were conditioned where necessary to prevent breakdown by ramping up and down from 0 to 600 V by smoothly rising and decreasing field several times, and then the measurements were carried out. Some of the doped samples did not need the ramping process. The separation between the electrodes is defined by the polytetrafluoroethylene (PTFE) spacer of thickness ~ 40 μ m, and the overlap area between the plate anode and cathode was kept at ~ 0.126 cm². The current-voltage (*I*-*V*) characteristics were measured at room temperature, in a vacuum greater than 7×10^{-6} mbar maintained by a turbopump-based vacuum system. In the case of field-emission study too, the maximum applied field over the gap (20 V/ μ m) was well below the breakdown voltage of the PTFE spacers (120–150 V/ μ m). Further after every measurement the samples were grounded to prevent any residual charges influencing the measured current. In order to verify if the currents were due to field emission, even before starting the actual measurements, the heavily doped uncoated silicon substrates and the PTFE spacer were used to study, if there was any influence of the substrate and the spacer on the emission process by ramping up the field to the maximum value of 20 V/ μ m. No measurable currents were observed in this range. Similarly we did not observe any measurable currents when the sample was measured in the reverse voltage conditions. The instrument was sensitive down to 1 pA only. These measurements were fairly repeatable and repro-

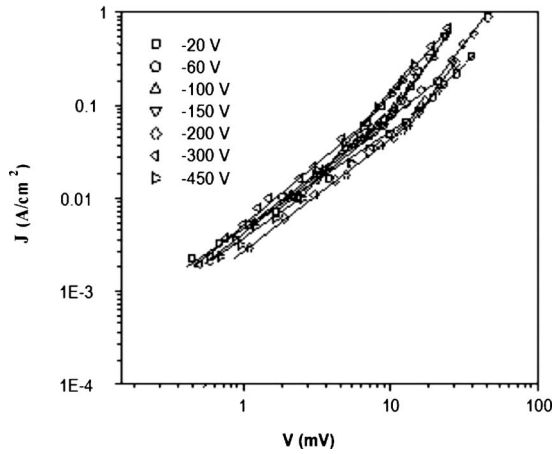


FIG. 1. Typical logarithmic J - V characteristics of $p^{++}\text{Si}/\text{ta-C}/\text{Al}$ structure for as-grown ta-C films deposited at different substrate biases.

ducible on the same sample at different locations and also on the samples prepared in the different runs under identical conditions. The emission current density (J) is calculated by dividing the current (I) by the area of the cathode, which is defined by the area of the hole in the spacer. The electric field (E) is obtained by voltage drop across the vacuum gap. Atomic force microscopy (AFM) (Digital Instruments, Nanoscope III) was used to study the morphology of the specimen at the micro-/nanolevel. The surface morphology was investigated in terms of surface profiles and surface roughness.

III. RESULTS AND DISCUSSION

A. As-grown ta-C films

1. SCLC measurements on as-grown ta-C films deposited at different substrate biases

The current density (J)-voltage (V) characteristics of the sandwiched structure of metal/ta-C/metal ($p^{++}\text{Si}/\text{ta-C}/\text{Al}$) were used to derive the information about the density of states in the gap. Figure 1 shows the typical logarithmic J - V characteristics made on $p^{++}\text{Si}/\text{ta-C}/\text{Al}$ at room temperature for as-grown ta-C films deposited using an S -bend FCVA process at different negative substrate biases. They are composed of two regions, which follow a power law of $J=V^m$,

with m being a constant. It may be noted that these curves begin with a linear Ohmic region with a slope (m) of about unity at lower voltage, followed by a gradual transition to a steeper curve with slope $m > 1.83$ ($1.83 < m < 2.72$), indicating the onset of SCLC at higher voltages. As-grown ta-C films deposited on silicon substrates have slopes of more than two because of the presence of traps in the films. No V^2 dependence, however, has been observed, as reported by Mackenzie *et al.*²⁹ This form of J - V characteristics cannot be explained by a single-trap model.³⁰ The density of the states [$N(E_F)$] was calculated from the J - V curves by the differential method of Nespurek and Sworakowski.³¹ In this analysis, $N(E_F)$ is related to the voltage V , and slope m ($=\partial \ln J / \partial \ln V$) of the experimental J - V curve is given by the following expression:^{31,32}

$$N(E_F) = [(a\varepsilon)/(ed^2kT)][V/(m-1)], \quad (1)$$

where a is a process-dependent constant that accounts for the nonuniformity of charge-carrier distribution and electric field within the space-charge region, which is taken to be 0.75; ε is the permittivity of the material, which is taken as 4.0×10^{-12} CV cm^{-1} for ta-C (DLC) films;³² e is the electronic charge; d is the thickness of the films; k is the Boltzmann constant; T is the temperature in kelvin; V is the voltage at which SCLC sets in. There is a sharp increase in the current with slope $m > 1.83$. The position of the quasi-Fermi level relative to $E_c=0$ is found by the following relation:

$$E_F = kT \ln(eN_c\mu_0 b/d) + kT \ln(V/J), \quad (2)$$

where the factor $eN_c\mu_0$ is a pre-exponential factor, μ_0 (carrier mobility) is obtained from the temperature dependence of the dc conductivity in the Ohmic region, b is a process-dependent constant with a value of 1.5 (assigned to account the non uniformity of the internal space-charge field), and N_c is the density of state at the conduction-band edge. The values of $N(E_F)$ calculated near the Fermi level for as-grown ta-C films deposited at different negative substrate biases are summarized in Table I. It is evident from the table that the value of $N(E_F)$ decreases in as-grown ta-C films deposited up to -200 V substrate bias and beyond -200 V substrate bias the value of $N(E_F)$ increases. Thus, the value of $N(E_F)$ is found to be a minimum (1.3×10^{17} cm^{-3} eV^{-1}) at -200 V substrate bias and it increases on either side of this bias volt-

TABLE I. $N(E_F)$ and emission parameters and of as-grown ta-C films deposited at different negative substrate biases.

Sample No.	Substrate bias (V)	$N(E_F)$ (cm^{-3} eV^{-1})	$E_{\text{turn-on}}$ (V/ μm)	J at 12.5 V/ μm (mA/ cm^2)	Slope m (V/m) $\times 10^6$	Φ (eV)	β	sp^3 (%) ^a
1	-20	3.3×10^{17}	9.5	0.60	128.06	0.12	257.83	49.4
2	-60	2.3×10^{17}	9.3	1.25	127.22	0.12	259.54	51.6
3	-100	2.0×10^{17}	8.7	1.28	109.15	0.11	302.51	59.9
4	-150	1.6×10^{17}	8.4	5.94	93.97	0.10	351.38	66.4
5	-200	1.3×10^{17}	8.3	6.19	90.23	0.10	365.94	79.8
6	-300	4.9×10^{17}	9.3	0.53	111.30	0.11	296.66	53.9
7	-450	1.7×10^{18}	9.9	0.18	145.83	0.13	226.42	35.5

^aReference 26.

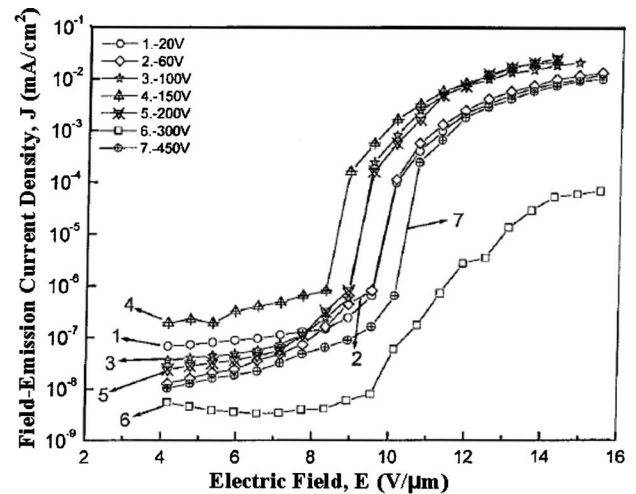
age. The values of $N(E_F)$ evaluated from SCLC measurements, reported by Veerasamy *et al.*³³ for ta-C films deposited by the FCVA process using an *L*-bend magnetic filter, are $\sim 5 \times 10^{17} \text{ cm}^{-3} \text{ eV}^{-1}$ at 0.22 eV from the valence-band edge because as-grown ta-C films are reported to be *p*-type and rises exponentially to $3 \times 10^{18} \text{ cm}^{-3} \text{ eV}^{-1}$ at 0.18 eV above the valence-band edge, where it becomes pinned. Thus, the values of $N(E_F)$ of as-grown ta-C film evaluated in the present study are consistent with the values of $N(E_F)$ of as-grown ta-C films deposited using the *L*-bend FCVA process reported by Veerasamy *et al.*³³ The minimum values of $N(E_F)$ are observed in as-grown ta-C films deposited at -200 V substrate bias, where the sp^3 content evaluated from XAES studies is found to be the maximum.²⁶ Fallon *et al.*¹ showed, using a FCVA system, that the optimal ion energy for the highest sp^3 -bonded fraction is close to $\sim 100 \text{ eV}$. This converts to an applied substrate bias of about 80 V based on the calculation that the as-generated carbon ion, in the case of a normal continuous cathodic arc, is $20\text{--}25 \text{ eV}$.³⁴ Thus, the substrate biases at which some of the properties go through a maximum or minimum are found to be system dependent.²

2. Field-emission measurements of as-grown ta-C films deposited at different negative substrate biases

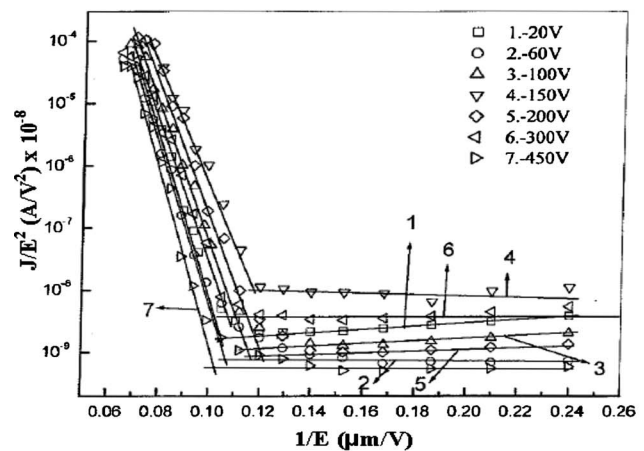
Figure 2(a) shows the variation in field-emission current density (J) versus electric field (E) characteristics for as-grown ta-C films deposited with different applied negative substrate biases. Field emission involves a quantum-mechanical process in which electrons tunnel out of the electrodes into vacuum when subjected to a very high electric field. It is a nonlinear process in which the J - E characteristics are usually described by the classical Fowler–Nordheim (FN) equation,³⁵

$$J = A[(\beta E)^2 / \varphi^{3/2}] \exp(-B\varphi^{3/2} / \beta E), \quad (3)$$

where J is the emission current density in A/cm^2 , φ is the barrier height in eV, E is the electric field in V/m , and β is the field-enhancement factor at sharp geometries. Terms A and B are constants, and the values of these constants are $A = 1.4 \times 10^{-2} \text{ A V}^{-2}$ and $B = 6.8 \times 10^9 \text{ V}/\text{meV}^{2/3}$, assuming that the effective mass of the field-emitted electron is equal to that of an electron at rest in the metal and vacuum. The plots of $\log(J/E^2)$ versus $1/E$ for the data shown in Fig. 2(a) are given in Fig. 2(b). These plots are straight lines, which confirm that the J - E characteristics follow the FN relation. The electric field corresponding to the point of inversion in the FN plot is defined as the threshold field of emission ($E_{\text{turn-on}}$). The slopes of these plots give the effective emission barriers (φ), if we assume an ideal plane emitter with a field-enhancement factor β of 1. The values of φ for ta-C films grown were in the range of $0.095\text{--}0.13 \text{ eV}$. Other workers³⁶ reported similar values of $0.019\text{--}0.044 \text{ eV}$. These values are obviously quite low, and the true barrier may be much larger.³⁷ If we take a work function (φ) of 5 eV , typical of graphite bonding, then the FN slopes correspond to the



(a)



(b)

Fig. 2. (a) Variation in field-emission current (J) vs electric field (E) characteristics of as-grown ta-C films deposited at different negative substrate biases and (b) FN plot of the as-grown ta-C films deposited at different negative substrate biases.

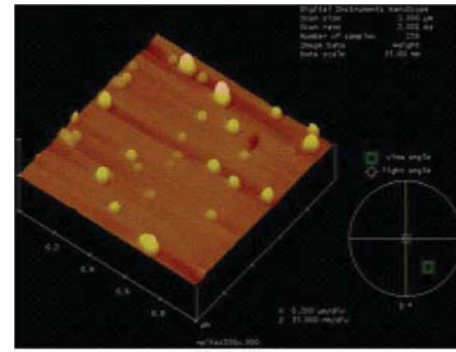
field-enhancement factor β of $226\text{--}366$ for these as-grown ta-C films. We understand that β , in the case of a parallel-plate arrangement and flat cathodes, is not a realistic estimation because emission is from discrete points. However, we wanted to see whether the estimated parameter, even though not accurate, correlates to some other calculated value or shows a consistent trend with a change in material properties with a change in process parameters. To understand the mechanism of electron emission, a realistic energy-band diagram of ta-C: N/n^{++} Si heterojunctions was proposed recently³⁷ from the experimentally measured valence- and conduction-band offsets, using *in situ* XPS and optical spectroscopy data. The values of φ of ta-C and ta-C: N films evaluated from this study are in the range of $3.95\text{--}4.55 \text{ eV}$.

The values of $E_{\text{turn-on}}$, J at $12.5 \text{ V}/\mu\text{m}$, slope m of FN plots, and β of ta-C films grown at different negative substrate biases are also summarized in Table I along with the value of $N(E_F)$ and sp^3 content evaluated.²⁶ It is evident

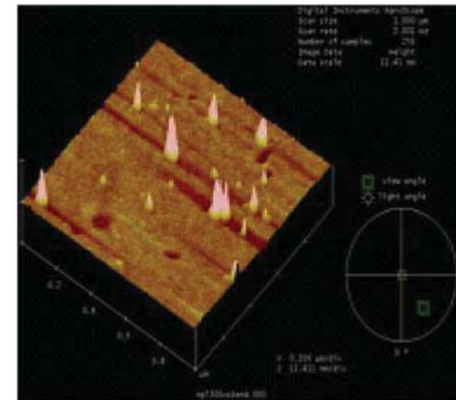
from Table I that the values of $E_{\text{turn-on}}$ and slope m decrease and those of J and β increase with the increase in substrate bias of up to -200 V. Beyond -200 V substrate bias, there is a reversal in the trend and the values of $E_{\text{turn-on}}$ and slope m increase and those of J and β decrease with the increase in substrate bias of up to -450 V. This trend is correlated with the trend of increase in sp^3 content²⁶ and decrease in $N(E_F)$ evaluated in Sec. III A 1 at different negative substrate biases of up to -200 V and a reversal in the trend occurs beyond -200 V substrate bias. We found that the ta-C films deposited at -200 V substrate bias have the highest value of sp^3 fraction (79.9%) evaluated from XAES study,²⁶ which is accompanied with the lowest value of $N(E_F)$ ($1.3 \times 10^{17} \text{ cm}^{-3} \text{ eV}^{-1}$) and these films show the lowest value of $E_{\text{turn-on}}$ of $8.3 \text{ V}/\mu\text{m}$, the smallest value of slope m of $90.23 \times 10^6 \text{ V/m}$ of FN plots, accompanied by the largest value of J of $6.19 \text{ mA}/\text{cm}^2$ at $12.5 \text{ V}/\mu\text{m}$ field and the largest value of β of 365.94 . This is found to be consistent with the report by Satyanarayana *et al.*,³⁶ who reported a decrease in $E_{\text{turn-on}}$ with an increase in sp^3 content but it is found to be opposite to the study reported by Wisitsora-at *et al.*³⁸ who reported lowering of $E_{\text{turn-on}}$ by increasing sp^2 content in diamond field emission using micropatterning of monolithic diamond tips with different sp^2 content. ta-C is a mixed phase material with sp^3 and sp^2 bonds whereas diamond has only sp^3 bonds so diamond tips with sp^2 content may show different behaviors. The minimum value of $E_{\text{turn-on}}$ of $8.3 \text{ V}/\mu\text{m}$ in ta-C films deposited at -200 V substrate bias using an *S*-bend FCVA process in the present study is somewhat lower than the 10 – $12 \text{ V}/\mu\text{m}$ obtained in ta-C films deposited using an *L*-bend FCVA system, at an ion energy of 80 – 100 eV , as reported by Satyanarayana *et al.*³⁶ This could also be due to some clustering occurring at high substrate bias.

3. AFM study of as-grown ta-C films

Figure 3 shows the typical three-dimensional AFM images of as-grown ta-C films deposited at (a) -200 V and (b) -300 V substrate biases. It is evident from the AFM image that the as-grown ta-C films deposited at -200 and -300 V substrate bias show root-mean-square (rms) roughnesses of ~ 2.06 and $\sim 1.15 \text{ nm}$, respectively, with grain diameters of ~ 1.19 and $\sim 0.60 \text{ nm}$, respectively. Li *et al.*,³⁹ while studying the sp^3/sp^2 ratio in ta-C films deposited by filtered arc deposition (FAD), reported that the sp^3 fraction attains a maximum 90% in ta-C films deposited at -200 V substrate bias and have low surface roughness of $\sim 0.11 \text{ nm}$. The rms roughness increases and sp^3 fraction decreases in either side of this bias voltage. The value of rms roughness of ta-C films deposited using the *S*-bend FCVA process observed in the present study is somewhat larger than the values reported in literature.³⁹ This could also be due to some clustering occurring at the high substrate bias.



(a)



(b)

Fig. 3. (Color online) Typical three-dimensional AFM images of as-grown ta-C films deposited at (a) -200 V and (b) -300 V substrate biases.

B. ta-C:H films

1. SCLC measurements on ta-C:H films deposited at different hydrogen partial pressures

Figure 4 shows the typical logarithmic J - V characteristics of a sandwiched structure ($p^{++}\text{Si}/\text{ta-C:H}/\text{Al}$) for ta-C:H films deposited at different hydrogen partial pressures ranging from 1.2×10^{-5} to $1.4 \times 10^{-3} \text{ mbar}$, maintaining a fixed substrate bias of -300 V. These curves begin with a linear Ohmic region with a slope of about unity, followed by a gradual transition to a steeper curve with slope $m > 2$ ($2.05 < m < 2.72$), indicating the onset of SCLC. The values of $N(E_F)$, calculated near the Fermi level, for ta-C:H films deposited at varying hydrogen partial pressures, from 1.2×10^{-5} to $1.4 \times 10^{-3} \text{ mbar}$, are summarized in Table II. It is evident from the table that hydrogen incorporation in ta-C films grown up to $3.4 \times 10^{-4} \text{ mbar}$ hydrogen partial pressure reduces the values of $N(E_F)$ continuously and saturates at $\sim 9.4 \times 10^{16} \text{ cm}^{-3} \text{ eV}^{-1}$. However, the value of $N(E_F)$ marginally increases to $1.5 \times 10^{17} \text{ cm}^{-3} \text{ eV}^{-1}$, for films grown at a maximum hydrogen partial pressure of $1.4 \times 10^{-3} \text{ mbar}$ used in this study. The values of $N(E_F)$ evaluated are consistent with the values of $N(E_F)$ of $6 \times 10^{16} \text{ cm}^{-3} \text{ eV}^{-1}$ at 0.3 eV above the valence band, as reported by Veerasamy *et al.*³³ for as-grown ta-C films deposited in an *L*-bend FCVA system. The values of $N(E_F)$, evaluated from SCLC mea-

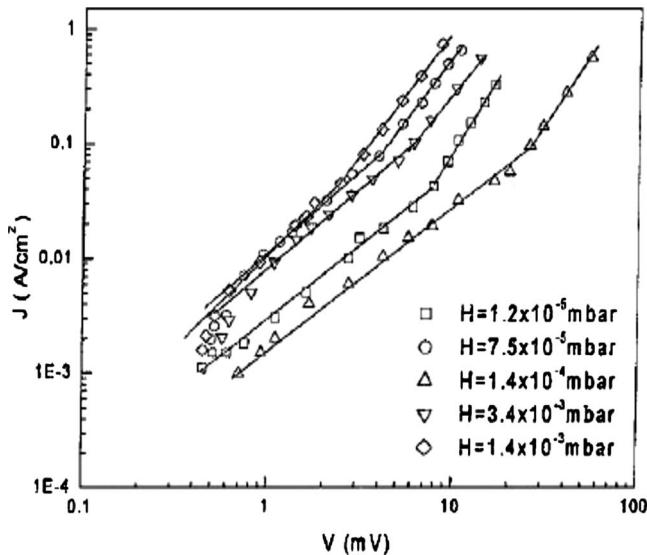
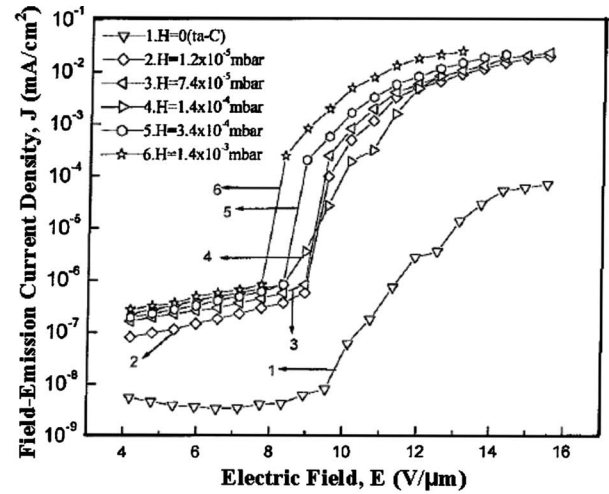
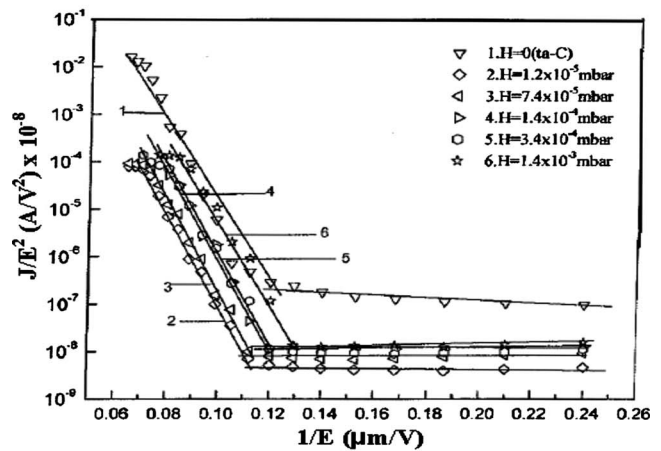


FIG. 4. Typical logarithmic J - V characteristics of $p^{++}\text{Si}/\text{ta-C:H}/\text{Al}$ structure for ta-C:H films deposited at different hydrogen partial pressures.

measurements, on $a\text{-C:H}$ films grown using CH_4 gas in a rf plasma chemical vapor deposition system by Silva and Amaratunga,³² are reported to be $8\text{--}9 \times 10^{17} \text{ cm}^{-3} \text{ eV}^{-1}$. In the case of mixed phase material with sp^2 and sp^3 bonds in relatively significant proportion, hydrogen has a significant role. For the case of lower energetic plasma process-grown $a\text{-C:H}$ (DLC) films, the hydrogen content is far higher than the more energetic ion-assisted process such as cathodic vacuum arc, but the energetic process may lead to a similar level of hydrogen incorporation. Hydrogen incorporation seems to be effective in reducing the density of localized states, specifically states that lie in the region of the quasi-Fermi level. Because the π bonds lie closest to the Fermi level, they control the electronic properties. The decrease in the value of $N(E_F)$ with the increase in hydrogen incorporation is accompanied with the increase in sp^3 content evaluated from XAES studies.²⁶ This is found to be consistent with the report by Silva and Amaratunga³² who reported reduction in the bulk density of states in ta-C:H or $a\text{-C:H}$ film due to a reduction in sp^2 fraction.³²



(a)



(b)

FIG. 5. (a) Variation in field-emission current (J) vs electric field (E) characteristics of ta-C:H films deposited with different hydrogen partial pressures and (b) FN plot of the ta-C:H films deposited at different hydrogen partial pressures.

2. Field-emission measurements of ta-C:H films with different hydrogen partial pressures

Figure 5(a) shows the variation of the field-emission current density (J) versus electric field (E) characteristics of

TABLE II. $N(E_F)$ and emission parameters of ta-C:H films deposited at different hydrogen partial pressures.

Sample No.	H partial pressure (mbar)	$N(E_F)$ ($\text{cm}^{-3} \text{ eV}^{-1}$)	$E_{\text{turn-on}}$ ($\text{V}/\mu\text{m}$)	J at $12.5 \text{ V}/\mu\text{m}$ (mA/cm^2)	Slope m ($\text{V}/\text{m}) \times 10^6$	Φ (eV)	β	sp^3 (%) ^a
1	0	4.9×10^{17}	9.3	0.53	111.30	0.11	296.66	53.9
2	1.2×10^{-5}	3.6×10^{17}	8.9	1.08	99.59	0.10	331.55	61.9
3	7.4×10^{-5}	1.5×10^{17}	8.8	1.94	97.89	0.10	337.30	62.3
4	1.4×10^{-4}	1.4×10^{17}	8.3	8.1	92.66	0.10	356.34	86.9
5	3.4×10^{-4}	9.4×10^{16}	8.2	21.4	89.64	0.10	368.34	80.0
6	1.4×10^{-3}	1.5×10^{17}	7.7	22.2	87.21	0.10	378.61	87.5

^aReference 26.

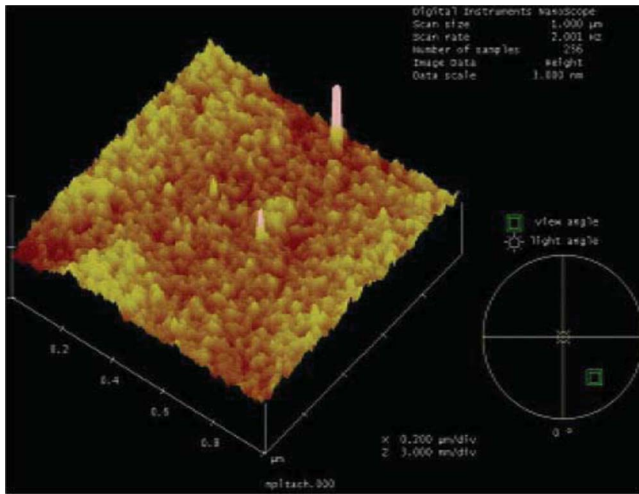


Fig. 6. (Color online) Typical three-dimensional AFM image of ta-C:H film deposited at 1.4×10^{-4} mbar hydrogen partial pressure.

ta-C:H films deposited with different hydrogen partial pressures, maintaining a fixed substrate bias of -300 V. The J - E characteristics follow the same FN equation and the plots of $\log(J/E^2)$ versus $1/E$, for the data points shown in Fig. 5(a) are given in Fig. 5(b). These plots are also straight lines, which confirm that J - E characteristics follow the same FN relation. The values of $E_{\text{turn-on}}$, J at 12.5 V/ μm , slope m of FN plots, and β for ta-C:H films deposited at different hydrogen partial pressures are summarized in Table II along with the value of N (E_F) and sp^3 content evaluated.²⁶ It is evident from Table II that hydrogen incorporation in as-grown ta-C films continuously reduces the values of $E_{\text{turn-on}}$, slope m of FN plots, and increases the values of J and β with the increase in hydrogen partial pressure used in depositing ta-C:H films. The value of ϕ evaluated for an ideal plane emitter with a field-enhancement factor of one in ta-C:H film remains the same at 0.10 eV and does not change with hydrogen incorporation. Other workers³⁶ also reported similar values. The decrease in $E_{\text{turn-on}}$ and slope m of FN plot, accompanied by the increase in J and β obtained in ta-C:H films deposited with an increase in hydrogen partial pressures, correlates with the trend of reduction in the value of N (E_F) evaluated in Sec. III B 1 and an increase in sp^3 content evaluated from the XAES study.²⁶ The lowest $E_{\text{turn-on}}$ (7.7 V/ μm) were observed in ta-C:H films deposited at a hydrogen partial pressure of 1.4×10^{-3} mbar, where the sp^3 content evaluated from XAES studies²⁶ was the maximum ($\sim 87\%$) and N (E_F) was minimum ($\sim 10^{17}$ cm $^{-3}$ eV $^{-1}$).

3. AFM study of ta-C:H films

Figure 6 shows the three-dimensional AFM image of ta-C:H film deposited at 1.4×10^{-4} mbar hydrogen partial pressure, maintaining a substrate bias of -300 V. The AFM image of ta-C:H films deposited at 1.4×10^{-4} mbar partial pressure shows the rms roughness value of ~ 0.56 nm, with a grain diameter of ~ 0.23 nm, which is less than the rms roughness value of ~ 1.15 nm with grain diameter of

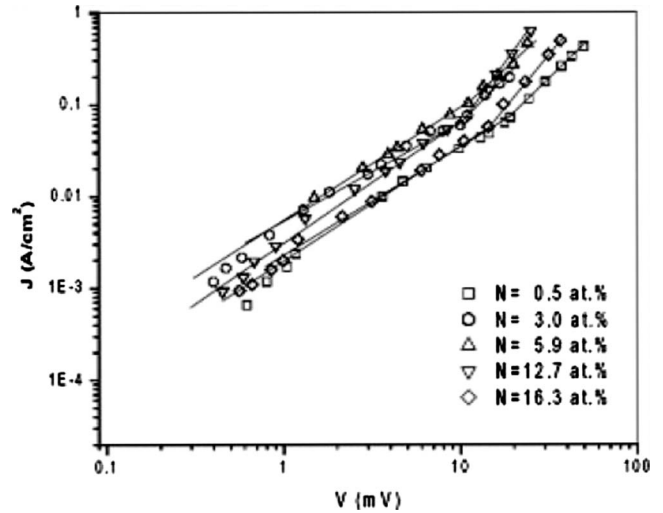


Fig. 7. Typical logarithmic J - V characteristics of $n^{++}\text{Si}/\text{ta-C:N}/\text{Al}$ structure for ta-C:N films deposited with different N contents.

~ 0.60 nm observed in as-grown ta-C films deposited at -300 V substrate bias. Thus, hydrogen incorporation in ta-C films appears to reduce the roughness and enhances the smoothness of the growing film. There is limited literature on the AFM study of ta-C:H films using cathodic arc for comparison purpose, except the study of DLC films deposited by microwave plasma enhanced chemical vapor deposition (MW PECVD) under varying bias voltage by Pandey *et al.*⁴⁰ They stated that the surface morphology, density, and sp^3/sp^2 ratio of these films are related to each other and follow the subplantation model. These authors reported that rms roughness decreased from ~ 3.16 to ~ 1.14 nm in DLC films as the bias voltage increased from -300 to -800 V. The rms roughness started to increase again and becomes ~ 1.30 and ~ 1.77 nm in DLC films deposited at -1000 and -1400 V substrate bias voltages, respectively.

C. ta-C:N films

1. SCLC measurements on ta-C:N films deposited at different nitrogen contents

Figure 7 shows the typical logarithmic J - V characteristics of a sandwiched structure ($n^{++}\text{Si}/\text{ta-C:N}/\text{Al}$) for ta-C:N films deposited using an S-bend FCVA process at different nitrogen contents ranging from 0.5 to 16.3 at. %, maintaining a fixed substrate bias of -300 V. These curves begin with a linear Ohmic region with a slope of about unity, followed by a gradual transition to a steeper curve with slope $m > 1.91$ ($1.91 < m < 2.56$), indicating the onset of SCLC. The values of N (E_F), calculated near the Fermi level, for ta-C:N films deposited with different N contents, ranging from 0.5 to 16.3 at. %, are summarized in Table III. It is evident from the table that a small amount of N incorporation in ta-C:N films up to 5.9 at. % N content reduces the value of N (E_F) to 8.0×10^{16} cm $^{-3}$ eV $^{-1}$. Beyond 5.9 at. % N content, the value of N (E_F) increases continuously and becomes 5.0×10^{17} cm $^{-3}$ eV $^{-1}$ in ta-C:N films deposited with 16.3 at. % N content. As-grown ta-C film is a p -type semiconductor

TABLE III. $N(E_F)$ and emission parameters of ta-C:N films deposited at different nitrogen contents.

Sample No.	N content (at. %)	$N(E_F)$ ($\text{cm}^{-3} \text{eV}^{-1}$)	$E_{\text{turn-on}}$ ($\text{V}/\mu\text{m}$)	J at $12.5 \text{ V}/\mu\text{m}$ (mA/cm^2)	Slope m ($\text{V}/\text{m}) \times 10^6$	Φ (eV)	β	sp^3 (%) ^a
1	0	4.9×10^{17}	9.3	0.53	111.30	0.11	296.66	53.9
2	0.5	4.2×10^{17}	8.8	1.76	101.24	0.11	326.13	78.3
3	3.0	2.3×10^{17}	8.4	4.47	96.64	0.10	341.65	83.7
4	5.9	8.0×10^{16}	8.1	8.41	96.20	0.10	343.22	75.5
5	12.7	1.3×10^{17}	7.8	17.50	92.40	0.10	357.36	86.4
6	16.3	5.0×10^{17}	7.6	23.70	88.76	0.10	371.38	90.6

^aReference 26.

with an optical gap of ~ 2 eV.⁴¹ The activation energy evaluated from the conductivity measurements is reported to rise systematically from the as-grown value of 0.22– ~ 1.0 eV above the valence band, with increasing nitrogen content up to 0.45%, and then decline to 0.12 eV below the conduction band as the nitrogen content is increased further.^{42,43} This effect is attributed to the movement of the Fermi level from close to the valence-band edge in the as-grown ta-C films to midgap, and then to a position close to the conduction-band edge. This behavior presumably indicates the substitutional dopant nature of nitrogen.^{42,43} It has been reported that for ta-C films grown under higher nitrogen partial pressure conditions to increase the nitrogen concentration, the enhanced deposition pressures tend to favor sp^2 cluster formation.²⁴ This indicates that sp^2 clustering leads to increased defect density. However to relatively minimize clustering and correspondingly reduce the defect density, in the current study the ion energy has been increased by using a higher negative bias. Nitrogen incorporation of up to 5.9 at. % N content passivates the p -type nature of as-grown ta-C films, and beyond 5.9 at. % N content the value of defect states increases and acts as n -type dopant in ta-C films. The trend of reduction in the values of $N(E_F)$ in ta-C:N films deposited up to 5.9 at. % N content correlates with the trend of increase in sp^3 content evaluated from XAES study²⁶ but beyond 5.9 at. % N content the value of $N(E_F)$ increases.

2. Field-emission measurements of ta-C:N films with different nitrogen contents

Figure 8(a) shows the variation of the field-emission current density (J) versus electric field (E) characteristics of ta-C:N films, deposited with different nitrogen contents, maintaining a fixed substrate bias of -300 V. The J - E characteristics follow the same classical FN equation, and the plots of $\log(J/E^2)$ versus $1/E$, for the data points shown in Fig. 8(a), are given in Fig. 8(b). These plots are also straight lines, which confirm that J - E characteristics follow the same FN relation. The values of $E_{\text{turn-on}}$, J at $12.5 \text{ V}/\mu\text{m}$, slope m of FN plots, and β for ta-C:N films with different N contents are summarized in Table III along with the values of $N(E_F)$ and sp^3 content evaluated.²⁶ The value of ϕ evaluated in ta-C:N film is 0.10–0.11 eV and does not seem to change with N incorporation. Similar values were reported by other workers.³⁶ The realistic values of ϕ (Ref. 37) evaluated in

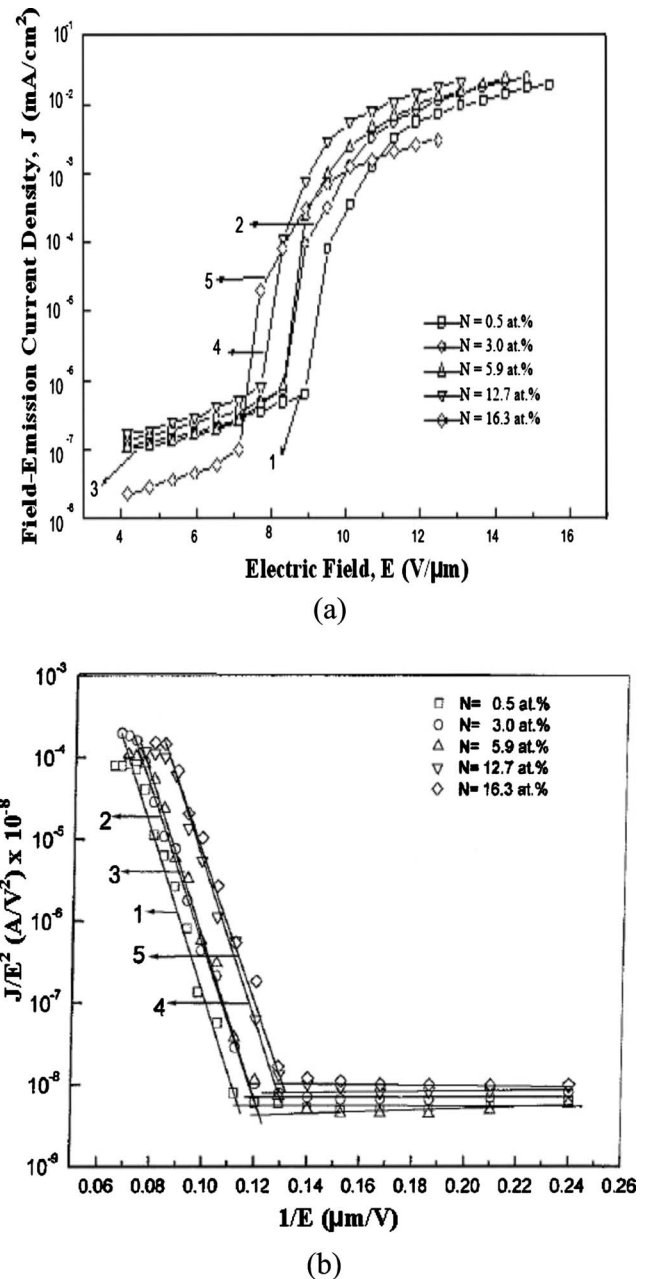


FIG. 8. (a) Variation in field-emission current (J) vs electric field (E) characteristics of ta-C:N films deposited with different N contents and (b) FN plot of the ta-C:N films deposited at different N contents.

ta-C:N films deposited by the pulsed FCVA technique with *L*-bend magnetic filter are in the range of 3.95–4.55 eV. It is evident from Table III that the values of $E_{\text{turn-on}}$ and slope m of FN plot decrease and those of J and β increase, with the increase in N content up to 16.3 at. % used in depositing these ta-C:N films. The decrease in $E_{\text{turn-on}}$ and slope m , accompanied by an increase in J and β obtained in ta-C:N films with an increased N content, correlates with the trend of increase in sp^3 content evaluated from XAES studies²⁶ and with the reduction in N (E_F) to some extent (up to 5.9 at. % N content) in the present study.

In general, nitrogen incorporation in DLC films leads to the following: (i) reduction in residual stress,^{44–46} (ii) reduction in optical band gap (E_g),⁴⁷ and (iii) enhancement of conductivity.⁴⁷ All these factors need to be carefully understood while discussing field emission for nitrogenated DLC films. However, the universality of stress reduction in nitrogen incorporation in the *a*-C:H network is well documented.^{44–46} The mechanism set forward to explain this behavior involves replacement of a fourfold-coordinated carbon by N atoms. As the N atoms admit a coordination number equal to at most three (sp^3 -hybridized N), the replacement of C atoms by N atoms in *a*-C:H film necessarily implies a reduction in the average coordination number. This, in turn, leads to the reduction in the degree of over constraint, and hence, reduction in internal residual stress in the films.⁴⁶

Satyanarayana *et al.*³⁶ studied field emission from ta-C films grown by the *L*-bend FCVA technique and reported that the values of $E_{\text{turn-on}}$ decrease with the increase in sp^3 content, as well as with low levels of N incorporation. They reported the minimum values of $E_{\text{turn-on}} = 10\text{--}12$ V/ μm for an ion energy around 80–100 eV in ta-C films and 3–5 V/ μm with the addition of $\sim 0.4\%$ N. Panwar *et al.*³⁷ reported that the nitrogen incorporation up to 5.2 at. % N content in ta-C films deposited using the pulsed FCVA technique with *L*-bend magnetic filter at 22 eV reduces the values of $E_{\text{turn-on}}$ from 9.9 to 5.3 V/ μm and increases the values of J from 4.8×10^{-7} to 2.1×10^{-4} A/cm²; beyond 5.2 at. % N content there is a reversal of the trend. It is stated that the properties investigated are found to be system dependent and may vary from laboratory to laboratory.² Amaratunga and Silva⁴⁸ also studied nitrogen-containing *a*-C:H films grown by the rf-PECVD technique with magnetic confinement. They reported that the onset emission-field decreases with the increase in N content, and an onset emission field as low as 4 V/ μm was obtained in *a*-C:H films having 15% N content. Weber *et al.*⁴⁹ reported an onset emission field as low as 3.2 V/ μm in *a*-C:N films with 0.6 at. % N content grown by sputtering of graphite employing an electron cyclotron resonance plasma as argon ion source. They achieved current densities up to 0.6 mA/cm² at an electric field of 5.8 V/ μm . However, the values of $E_{\text{turn-on}}$ obtained in these ta-C:N films deposited with different N contents in the present study are larger than the values of $E_{\text{turn-on}}$ obtained by Satyanarayana *et al.*³⁶ in ta-C:N films deposited at 80–100 eV ion energy using the *L*-bend FCVA process. The

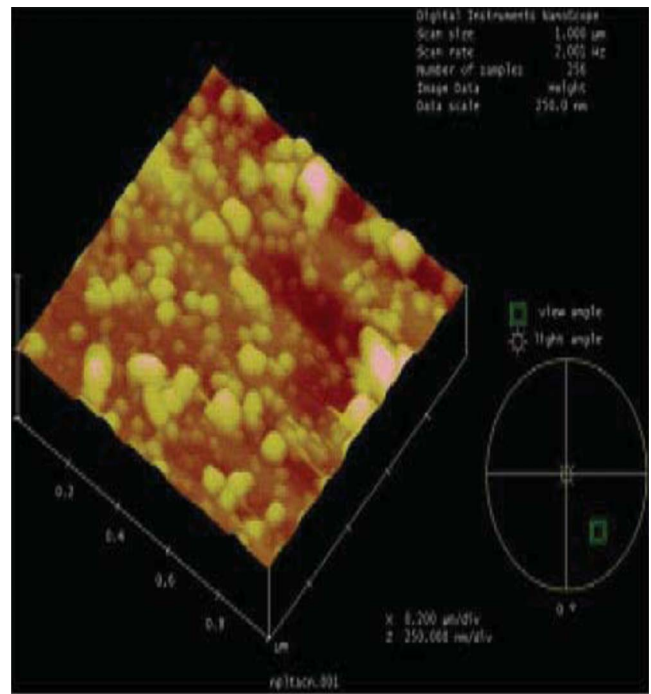


Fig. 9. (Color online) Typical three-dimensional AFM image of ta-C:N film deposited with 12.7 at. % N content.

values of current density obtained in these ta-C:N films are larger than the values of current density obtained by Satyanarayana *et al.*³⁶ and Panwar *et al.*,³⁷ grown by a pulsed FCVA technique with an *L*-bend magnetic filter.

3. AFM study of ta-C:N films

Figure 9 shows the three-dimensional AFM image of ta-C:N films deposited with 12.7 at. % N content, maintaining a fixed substrate bias of -300 V. The AFM image of ta-C:N film shows rms roughness of ~ 4.89 nm with a grain diameter of ~ 3.73 nm, which is much larger than the rms roughness of ~ 1.15 nm and grain diameter of ~ 0.60 nm observed in as-grown ta-C films deposited at -300 V substrate bias. Thus, nitrogen incorporation in ta-C:N films significantly increased the rms roughness and this is consistent with reports by Satyanarayana *et al.*²⁴ and Arena *et al.*⁵⁰ Chen *et al.*,⁵¹ while studying the surface morphology of nitrogen-doped ta-C films deposited by the FCVA process, observed the opposite and reported that the surface is uniform and smooth on the nanometer scale and N-doped ta-C films have rms roughness of 0.25–0.26 nm, which is larger than the rms roughness of 0.23 nm for undoped ta-C films.

D. Comparison of results obtained with those existing in literature and models

The contributions to field emission from a semiconductor surface are from electrons from the conduction band, valence band, and/or surface states. The field emission depends on the following: (i) the nature of the substrate material, (ii) the film, and (iii) the surface of the film.⁵² This implies that the silicon substrates maintain a supply of electrons into the

DLC layer, and these electrons are then transported through the DLC layer; finally, the electrons tunnel from the surface of the DLC layer into the vacuum, completing the field emission. For better performance, steps (ii) and (iii) mentioned above require the deposition parameters of the DLC films to be chosen in such a way so that field emission from the DLC layer can be maximized at low turn-on fields. A satisfactory field-emission behavior of the DLC films can probably be expected from the presence of both graphitic and diamond-carbon components. There may also be an optimum abundance ratio and connectivity of the network of diamond and graphitic carbon in the DLC films, where these films may perform as better field emitters. Gupta *et al.*,⁵³ while studying the electron field-emission and microstructure correlation in nanocrystalline carbon thin films, stated that along with grain size and optical band gap dependence, the defects (specially localized states within the band gap of nanocrystalline carbon thin films) where transport of electrons occurs through a hopping mechanism play a crucial role and assist in lowering emission threshold. We reported⁵⁴ a correlation of threshold field required for emission in DLC films grown by various techniques on residual stress, optical band gap (E_g), and characteristic energy of band tails (Urbach energy, E_0), and the values of threshold field of electron emission decrease with the decrease in residual stress, E_g , and E_0 as well. It is also evident from the present study that large emission current density and low emission threshold are obtained in those films that have low density of states and high sp^3 content. We have, thus, attempted to correlate the density of states evaluated from the SCLC data and field-emission properties and understand the feasibility of using the high-substrate-bias-grown carbon material by cathodic arc process as an interesting material for electronic devices and sensor based applications. These results appear to be the first on such high substrate bias samples, which need to be studied further.

Comparing our experimental results with previous works, we find that the values of $E_{\text{turn-on}}$ of ta-C films reported in this article are lower than the values obtained by Park *et al.*,⁵⁵ Chuang *et al.*,⁵⁶ Missert *et al.*,⁵⁷ and significantly lower than those of undoped *a*-C:H film.⁵⁸ These values are larger to those reported for similar material by Satyanaryana *et al.*,³⁶ or for nitrogen-containing carbon films reported by Amaratunga and Silva,⁴⁸ Weber *et al.*,⁴⁹ and Panwar *et al.*³⁷ grown under different process conditions.

A space-charge-induced band bending and hot-electron transport model was proposed by Amaratunga and Silva⁴⁸ to explain low electron field-emission from *a*-C:H:N thin films. They suggested that electrons from the back contact enter the *a*-C films (via tunneling or thermal excitation), under the influence of an internal applied electric field and gain enough energy during transport in the depleted *a*-C:H:N space-charge region to surmount the relatively low barrier ($\sim 2-3$ eV) for emission into vacuum. Forrest *et al.*⁵⁹ argued that their observation of minimum threshold field for electron emission, at an optimal thickness, can be best explained by the space-charge-induced band-bending model.⁴⁸

Zhao *et al.*,⁶⁰ however, reported thickness-independent electron field emission from ta-C films grown by FAD. In contrast, Hart *et al.*⁶¹ found no correlation between threshold voltage and the work function of the back contact for field emission from ta-C films deposited on various metals. Robertson⁶² argued, using photoemission data from *a*-C:H, that the primary barrier lies at the front surface of the films. He proposed that electron emission from *a*-C films occurs due to a large variation in the electron affinity in C-H-terminated and unterminated surface regions, causing the electric field from the anode to be concentrated at the unhydrogenated areas. The focusing of the electric field on the negative charges results in downward band bending, allowing electron emission via the FN process,³⁵ without exceeding the thermal breakdown field. Panwar *et al.*,³⁷ while reporting field-emission measurements on as-grown ta-C and nitrogen-incorporated ta-C films grown by a pulsed FCVA technique with *L*-bend magnetic filter, stated that using a realistic energy-band diagram proposed for ta-C:N/ n^{++} Si heterojunction, a barrier exists to the emission. They further observed that the main barrier lies at the front surface, which is related to the conduction-band offset. A number of other models have also been proposed in literature based on negative electron affinity,⁶³ defect bands in diamond,⁶⁴ surface dipole-controlled emission,⁶⁵ and field enhancement due to surface features.⁶⁶ Although they can be used to fit some emission data from different types of films, none of them is universally acceptable. We think that the electron field-emission still could be explained by the classical FN theory and also on density of states, microstructure, and sp^3/sp^2 ratio dependence. Certainly, a debate on emission mechanism exists; therefore, further study is needed to develop and modify the present models or to build new ones. It may also be noted that despite several detailed studies on ta-C-related material³ and their field-emission studies^{6,7} available in literature, some pitfalls in amorphous carbon studies still exist.² However the current study clearly indicates that the defect density, the sp^3/sp^2 bonding, possibly the nanocluster dimension (as envisaged from surface roughness) and the corresponding field assisted electron emission properties could all be controlled. Thus, the study shows the possibility of using higher energy (higher negative substrate bias) process-grown ta-C or associated mixed phase nanocarbons using Cathodic arc process could be an interesting electronic material with significant applications as sensors, MEMS, and large area microelectronics and flexible electronics.

IV. CONCLUSION

We have reported one of the first detailed study of defect density and field assisted electron emission from hydrogen and nitrogen-incorporated ta-C films grown at high substrate bias (-300 V) and also the influence of substrate bias on as deposited ta-C films, using an *S*-bend filtered cathodic vacuum arc process. The relatively low values of electronic defect density [$N(E_F) = 8.0 \times 10^{16} \text{ cm}^{-3} \text{ eV}^{-1}$], field assisted electron emission threshold ($E_{\text{turn-on}} = 7.6 \text{ V}/\mu\text{m}$), and a corresponding higher emission current density (J

=23.7 mA/cm²) during varying conditions of hydrogen and nitrogen incorporation in ta-C films grown at higher substrate bias (−300 V) clearly shows that there is a further scope to tailor ta-C as an electronic material by further studying and optimizing the process parameters and substrate bias could be a very critical parameter. The electron field-emission data are explained by using the Fowler–Nordheim theory and are found to depend on the sp^3/sp^2 ratio, microstructure, and density of states of these films. Large emission current density and low emission threshold are obtained in those films that have low density of states and high sp^3 content with optimum sp^2 matrix interconnect. Thus, the study shows the possibility of using higher energy (higher negative substrate bias) as an interesting route to ta-C or associated mixed phase nanocarbons grown using the Cathodic arc process as a useful material for electronics and sensor application and especially for large area and flexible electronics.

ACKNOWLEDGMENTS

The authors are grateful to the Director, National Physical Laboratory, New Delhi (India), for his kind permission to publish this article. They wish to thank P. N. Dixit, C. M. S. Rauthan, and Abhilasha Chouksey for their help and useful discussion. M.A.K. is grateful to the Ministry of Science and Technology, Government of India, and the Council of Scientific and Industrial Research, Government of India for providing the financial assistance during the course of this work. Ishpal is grateful to the Ministry of Science and Technology, Government of India, for providing the financial assistance.

- ¹P. J. Fallon, V. S. Veerasamy, C. A. Davis, J. Robertson, G. A. J. Amaratunga, W. I. Milne, and J. K. Koskinen, *Phys. Rev. B* **48**, 4777 (1993).
- ²Y. Lifshitz, *Diamond Relat. Mater.* **12**, 130 (2003).
- ³J. Robertson, *Mater. Sci. Eng. R.* **37**, 129 (2002).
- ⁴D. R. McKenzie, *Rep. Prog. Phys.* **59**, 1611 (1996).
- ⁵A. Grill, *Diamond Relat. Mater.* **12**, 166 (2003).
- ⁶J. T. H. Tsai, K. B. K. Teo, and W. I. Milne, *J. Vac. Sci. Technol. B* **20**, 1 (2002).
- ⁷N. S. Xu and S. E. Huq, *Mater. Sci. Eng. R.* **48**, 47 (2005).
- ⁸A. Vaseashta and D. D. Malinowska, *Sci. Technol. Adv. Mater.* **6**, 312 (2005).
- ⁹Y. Lifshitz, *Diamond Relat. Mater.* **8**, 1659 (1999).
- ¹⁰R. L. Boxman, V. Zhitomirsky, B. Alterkop, E. Gidalevich, I. Beilis, M. Keider, and S. Goldsmith, *Surf. Coat. Technol.* **86–87**, 243 (1996).
- ¹¹I. I. Aksenov, V. A. Belou, V. G. Padalka, and V. M. Khoroshikh, *Sov. Phys. Tech. Phys.* **4**, 428 (1978).
- ¹²X. Shi, B. K. Tay, H. S. Tan, L. Zhong, Y. Q. Tu, S. R. P. Silva, and W. I. Milne, *J. Appl. Phys.* **79**, 7234 (1996).
- ¹³S. Xu, D. Flynn, B. K. Tay, S. Praver, K. W. Nugent, S. R. P. Silva, Y. Lifshitz, and W. I. Milne, *Philos. Mag. B* **76**, 351 (1997).
- ¹⁴X. Shi, B. K. Tay, and S. P. Lau, *Int. J. Mod. Phys. B* **14**, 136 (2000).
- ¹⁵S. Anders, A. Anders, M. R. Dickinson, R. A. MacGill, and I. G. Brown, *IEEE Trans. Plasma Sci.* **25**, 670 (1997).
- ¹⁶A. Anders and A. V. Kulkarni, *Mater. Res. Soc. Symp. Proc.* **675**, W 11.1 (2001).
- ¹⁷M. C. Polo, J. L. Andujar, A. Hart, J. Robertson, and W. I. Milne, *Diamond Relat. Mater.* **9**, 663 (2000).
- ¹⁸T. Schuelke, T. Witke, H. J. Scheibe, P. Siemroth, B. Schultrich, O. Zimmer, and J. Vetter, *Surf. Coat. Technol.* **120–121**, 226 (1999).
- ¹⁹A. Anders, W. Fong, A. V. Kulkarni, F. W. Ryan, and C. S. Bhatia, *IEEE Trans. Plasma Sci.* **29**, 768 (2001).
- ²⁰E. Alakoski, M. Kiuru, V. M. Tiainen, and A. Anttila, *Diamond Relat. Mater.* **12**, 2115 (2003).
- ²¹B. S. Satyanarayana, H. Takahashi, T. Narusawa, and A. Hiraki, *Mater. Res. Soc. Symp. Proc.* **675**, W10.2 (2001).
- ²²A. Hiraki and B. S. Satyanarayana, *IEICE Trans. Electron.* **86-C**, 816 (2003).
- ²³B. Schultrich, H. J. Scheibe, and H. Mai, *Adv. Eng. Mater.* **2**, 419 (2000).
- ²⁴B. S. Satyanarayana, J. Robertson, and W. I. Milne, *J. Appl. Phys.* **87**, 3126 (2000).
- ²⁵O. S. Panwar, M. Alim Khan, B. Bhattacharjee, A. K. Pal, B. S. Satyanarayana, P. N. Dixit, R. Bhattacharyya, and M. Y. Khan, *Thin Solid Films* **515**, 1597 (2006).
- ²⁶O. S. Panwar, M. Alim Khan, Mahesh Kumar, S. M. Shivaprasad, B. S. Satyanarayana, P. N. Dixit, R. Bhattacharyya, and M. Y. Khan, *Thin Solid Films* **516**, 2331 (2008).
- ²⁷O. S. Panwar, M. Alim Khan, P. N. Dixit, B. S. Satyanarayana, R. Bhattacharyya, Sushil Kumar, and C. M. S. Rauthan, *Indian J. Pure Appl. Phys.* **46**, 255 (2008).
- ²⁸O. S. Panwar, M. Alim Khan, G. Bhagavanarayana, P. N. Dixit, Sushil Kumar, and C. M. S. Rauthan, *Indian J. Pure Appl. Phys.* **46**, 797 (2008).
- ²⁹K. D. Mackenzie, P. G. Le Comber, and W. E. Spear, *Philos. Mag. B* **46**, 377 (1982).
- ³⁰M. A. Lampert and P. Mark, *Current Injection in Solids* (Academic, New York, 1970).
- ³¹G. W. Nespurek and J. Sworakowski, *J. Appl. Phys.* **51**, 2098 (1980).
- ³²S. R. P. Silva and G. A. J. Amaratunga, *Thin Solid Films* **253**, 146 (1994).
- ³³V. S. Veerasamy, G. A. J. Amaratunga, C. A. Davis, W. I. Milne, P. Hewitt, and M. Weiler, *Solid-State Electron.* **37**, 319 (1994).
- ³⁴W. D. Davis and H. C. Miller, *J. Appl. Phys.* **40**, 2212 (1969).
- ³⁵R. H. Fowler and L. W. Nordheim, *Proc. R. Soc. London, Ser. A* **119**, 173 (1928).
- ³⁶B. S. Satyanarayana, A. Hart, W. I. Milne, and J. Robertson, *Appl. Phys. Lett.* **71**, 1430 (1997).
- ³⁷O. S. Panwar, Nalin Rupesinghe, and G. A. J. Amaratunga, *J. Vac. Sci. Technol. B* **26**, 566 (2008).
- ³⁸A. Wisitsora-at, W. P. Kang, J. L. Davidson, and D. V. Kerns, *Appl. Phys. Lett.* **71**, 3394 (1997).
- ³⁹W. J. Li, Z. R. Song, Y. H. Yu, X. Wang, S. C. Zou, and D. S. Shen, *J. Appl. Phys.* **94**, 284 (2003).
- ⁴⁰M. Pandey, D. Bhattacharyya, D. S. Patil, K. Ramachandran, and N. Venkatramani, *Surf. Coat. Technol.* **182**, 24 (2004).
- ⁴¹G. A. J. Amaratunga, D. E. Segal, and D. R. McKenzie, *Appl. Phys. Lett.* **59**, 69 (1991).
- ⁴²V. S. Veerasamy, J. Yuan, G. A. J. Amaratunga, W. I. Milne, K. W. R. Gilkes, M. Weiler, and L. M. Brown, *Phys. Rev. B* **48**, 17954 (1993).
- ⁴³V. S. Veerasamy, G. A. J. Amaratunga, C. A. Davis, A. E. Timbs, W. I. Milne, and D. R. McKenzie, *J. Phys.: Condens. Matter* **5**, L169 (1993).
- ⁴⁴C. J. Trong, J. M. Siverten, J. H. Judy, and C. Chand, *J. Mater. Res.* **5**, 2590 (1990).
- ⁴⁵C. A. Davis, D. R. McKenzie, Y. Yin, E. Kravtchinskaiia, G. A. J. Amaratunga, and V. S. Veerasamy, *Philos. Mag. B* **69**, 1133 (1994).
- ⁴⁶D. F. Franceschini, C. A. Achete, and F. L. Freire, *Appl. Phys. Lett.* **60**, 3229 (1992).
- ⁴⁷O. Amir and R. Kalish, *J. Appl. Phys.* **70**, 4958 (1991).
- ⁴⁸G. A. J. Amaratunga and S. R. P. Silva, *Appl. Phys. Lett.* **68**, 2529 (1996).
- ⁴⁹A. Weber, U. Hoffman, and C. P. Klages, *J. Vac. Sci. Technol. A* **16**, 919 (1998).
- ⁵⁰C. Arena, B. Kleinsorge, J. Roberson, W. I. Milne, and M. E. Welland, *J. Appl. Phys.* **85**, 1609 (1999).
- ⁵¹Z. Y. Chen *et al.*, *Mater. Lett.* **34**, 1 (1998).
- ⁵²J. S. Shim, E. J. Chi, H. K. Baik, and S. M. Lee, *J. Appl. Phys.* **37**, 440 (1998).
- ⁵³S. Gupta, B. L. Weiss, B. R. Weiner, and G. Morell, *J. Appl. Phys.* **89**, 5671 (2001).
- ⁵⁴O. S. Panwar, Sushil Kumar, S. S. Rajput, Rajnish Sharma, and R. Bhattacharyya, *Vacuum* **72**, 183 (2004).
- ⁵⁵K. C. Park, J. H. Moon, S. J. Chung, J. Jang, M. H. Oh, and W. I. Milne, *Appl. Phys. Lett.* **70**, 1381 (1997).
- ⁵⁶F. Y. Chuang, C. Y. Sun, H. F. Cheng, W. C. Wang, and I. Lin, *Appl. Surf. Sci.* **113–114**, 259 (1997).
- ⁵⁷N. Missert, T. A. Friedmann, J. P. Sullivan, and R. G. Copeland, *Appl. Phys. Lett.* **70**, 1995 (1997).
- ⁵⁸K. R. Lee, K. Y. Eun, S. Lee, and D. R. Jeon, *Thin Solid Films* **290–291**,

- 171 (1996).
- ⁵⁹R. D. Forrest, A. P. Burden, S. R. P. Silva, L. K. Cheah, and X. Shi, *Appl. Phys. Lett.* **73**, 3784 (1998).
- ⁶⁰J. P. Zhao, Z. Y. Chen, X. Wang, T. S. Shi, and T. Yano, *Appl. Phys. Lett.* **76**, 191 (2000).
- ⁶¹A. Hart, B. S. Satyanarayana, W. I. Milne, and J. Robertson, *Appl. Phys. Lett.* **74**, 1594 (1999); *Diamond Relat. Mater.* **8**, 809 (1999).
- ⁶²J. Robertson, *J. Vac. Sci. Technol. B* **17**, 659 (1999).
- ⁶³Z. H. Huang, P. H. Cutler, N. M. Miskovsky, and T. E. Sullivan, *Appl. Phys. Lett.* **65**, 2562 (1994).
- ⁶⁴W. Zhu, G. P. Kochanski, S. Jin, L. Seibles, D. C. Jacobson, M. McCormack, and A. E. White, *Appl. Phys. Lett.* **67**, 1157 (1995).
- ⁶⁵J. Robertson, *Mater. Res. Soc. Symp. Proc.* **498**, 197 (1998).
- ⁶⁶A. A. Talin, T. E. Felter, T. A. Freidmann, J. P. Sullivan, and M. P. Siegel, *J. Vac. Sci. Technol. A* **14**, 1719 (1996).